Simulating nonlinear optics in an ultrafast photoinjector

Shea A. Charkowsky [a]
Sergio Carbajo [b,1], Randy Lemons [b,c,2], Melina Endsley [c,3]

[a] *California Polytechnic State University, San Luis Obispo, CA, USA*
[b] *Linac Coherent Light Source Department, SLAC National Accelerator Laboratory, Stanford, CA, USA*
[c] *Colorado School of Mines, Golden, CO, USA*

Last revised: August 20, 2021.

A B S T R A C T

The Linac Coherent Light Source (LCLS) at SLAC National Accelerator Laboratory generates high-energy X-ray bursts using electrons ejected from copper by ultrafast UV laser pulses, whose shape in time influences the X-rays' quality and power. The photoinjector system producing the UV pulses (a) first initiates two infrared pulses, (b) shapes both in time, and then (c) focuses them onto a nonlinear optical crystal, which (d) combines their waveforms to produce green pulses, and this green light (e) passes through a second crystal, producing the UV pulses. In this work, a 2-spatial-dimensional MATLAB simulation of Steps (c) and (d) is made operational, expanded in functionality, and compared to the previous 1-dimensional version. Optical effects not seen in the 1D output are captured in the 2D by more comprehensive models and improved visualization functions, and obstructing interference is removed via back calculation from segmented portions of the far field pattern. The 1D and 2D models produce similar outputs but only after segmentation and back calculation.

1. Introduction

X-ray free electron lasers (XFELs) produce among the brightest and shortest laser pulses available to date. Bursts of high-energy x-rays on the order of femtoseconds (10^{-15} s) in duration can capture images of atomic processes occurring in real time.[1] In an XFEL, an electron bunch is accelerated to relativistic speeds and passed through an array of alternating magnets; this causes the electrons to oscillate and produce extremely intense coherent X-rays for use by experiments. In the Linac Coherent Light Source (LCLS) at SLAC, this process begins at the *photoinjector*, whose ultrashort UV laser pulses inject electrons from copper into the accelerator via the photoelectric effect. These UV pulses must be extremely short and should be as close to rectangular in time as possible in order to yield the highest quality X-rays.

Achieving ultrashort pulses such as these is more than a matter of toggling a shutter or modulating a power source. Instead, waves of varying frequency are initiated together, and the resulting interference acts as a Fourier series, which can create pulse shapes that are impossible using methods employed on a single frequency. A set of frequencies can be generated by the modes of the light's electric field in a fixed cavity, a technique called mode locking. Using this method, pulses as short as a few wavelengths of light can be produced. In our case, pulses have a duration of a few hundred femtoseconds.

These pulses can then be further modified by shifting the phases of these underlying frequencies. Achieving the shortest pulse possible requires that all of the phases be aligned, but we are interested in a longer pulse with a rectangular profile. Using acousto-optic modulation, i.e. dispersing light passing through a crystal using sound, these phases can be modified in order to add temporal dispersion to the beam. Phase shift can be represented as a function of frequency, often described by its Taylor expansion, of which different orders create distinct effects in the dispersed light:

- 0^{th} order: *Shifts the carrier envelope phase.* Intensity envelope is effectively unchanged.
- 1^{st} order: *Delays entire wave in time.* Intensity envelope shifted but undistorted.
- 2^{nd} order: *Linear with respect to frequency.* Intensity envelope is symmetrically stretched in time.
- 3^{rd} order: *Quadratic with respect to frequency.* Intensity envelope is skewed and develops smaller undulations.

Usually, 4^{th} order and higher effects are negligible, an assumption we make for the purposes of this research. By modifying 2^{nd} and 3^{rd} order phase oppositely in two pulses, we can approximate a rectangular pulse from the original Gaussian input beam.

Another difficulty is that due to the discrete electron energy levels on which stimulated emission depends for the function of a laser, the pulses here are not generated in UV outright; they are first produced from IR light of wavelength 1030 nm and then passed through optical crystals that upconvert the light to double its frequency, or 515 nm wavelength. In these crystals, if two photons are absorbed by

---

[1] Ph.D. in Physics, supervisor
[2] Ph.D. student, supervisor
[3] Undergraduate student, fellow researcher

the same electron before the electron returns to ground state, the electron will emit a single photon having the sum of the energies of the previous two, which corresponds to a sum of frequencies according to the Planck relation ($E = h\nu$). This is called *sum frequency generation* (SFG), and the more specific *second harmonic generation* (SHG) occurs when photons of the same frequency, especially when they are part of the same beam, experience SFG. These processes depend nonlinearly on the field energy and are thus studied in *nonlinear optics*. Crystals exhibiting this property are called *nonlinear crystals*.

With this background established, we can now examine the photoinjector system. It consists of the following components:

1. *A laser* emitting modelocked IR light
2. *A beam splitter*, which creates two pulses
3. *An acousto-optic modulator* (the Dazzler from Fastlite, in our case), which applies phase shifts separately to each input pulse
4. *A lens* to focus the pulses to the same point in space
5. *A nonlinear crystal* at the lens' focal point, which combines the pulses' waveforms via SFG
6. *A second nonlinear crystal*, which applies SHG to achieve the UV pulses

By applying opposite phase shifts to the input beams, it is possible to combine and filter them to produce roughly rectangular pulses (Figure 1). When the two non-collinear beams enter the crystal, several beams exit, but only the central beam is converted into UV for use by the photoinjector.

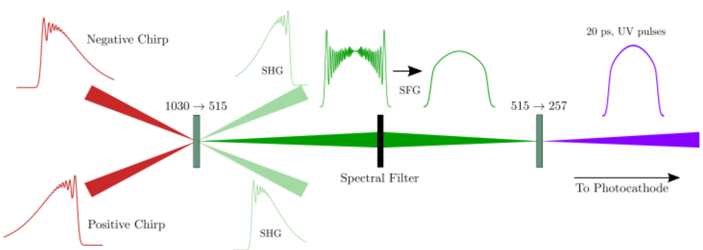

Figure 1. Nonlinear interactions within photoinjector, Steps 4-6.[2] Two phase-shaped IR pulses enter the first crystal, which creates multiple beams of green light via SFG. Note that the opposing shapes of the IR beams combine to a symmetric, roughly rectangular shape in the central green beam. A filter removes noise from that beam, and it is sent through a second crystal to create UV pulses via SHG.

The photoinjector's many parameters can each influence the resulting X-rays outputted by the LCLS. Our overarching goal is model this system in software and optimize these parameters via machine learning. In this specific work, we began with pre-existing 1- and 2-spatial-dimensional models of Step 4 in MATLAB. The 1D was well-established, but the 2D code had incorrect calculations and lacked organization. The aim for this work was to correct the 2D code and compare its outputs to the 1D in order to obtain a more comprehensive model of the optical processes involved. Once the 2D code is completed and tested, we will have increased confidence in its accuracy as a part of the larger eventual photoinjector simulation.

2. Methods

2.1 Simulation overview

Both the 1D and 2D code simulate the following:

A. Two initial Gaussian pulses
B. Phase shifts on those pulses
C. The behavior of light incident on the crystal
D. The behavior of light as it propagates in the crystal

There are a few important differences between the 1D and 2D models. First, in the 2D code, Step C involves focusing the pulses through a lens, so that the beams are not necessarily collinear. In the 1D, the light is assumed to be collinear and there is no lens. Second, the 2D code calculates SFG between the two input beams but also calculates SHG within each beam, whereas the 1D only calculates SFG between the two beams. Third, the 2D includes the calculation of the *far field pattern* after Step D, which is the intensity pattern that the light would create on a hypothetical screen positioned one focal length after the crystal (Figure 2); since the far field pattern involves a transverse dimension, it can only exist in the 2D model.

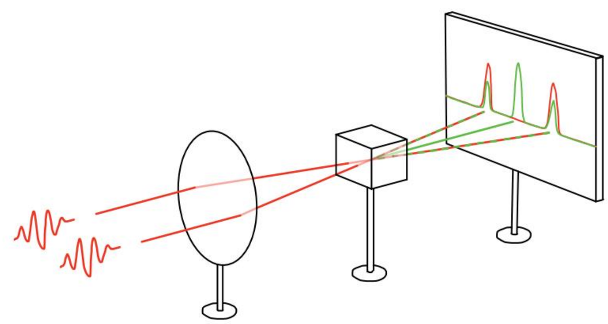

Figure 2. Pictorial of scope of 2D model, with far field pattern shown (right). Two IR beams enter the lens, focus on the crystal, and pass through. As they do, SFG and SHG occur, respectively yielding the central green peak and off-center green peaks of the far field pattern.

Propagation in Step D employs a *split-step Fourier method*, a numerical solution that at each spatial step advances the light in the frequency domain and then solves for nonlinear optical effects in the time domain, and this process repeats through the crystal's length.[3] The time and frequency profiles of the electric field phasors for both the IR and green light at every point in the crystal are stored in a single array that forms the basis for all visualizations of light behavior within the crystal.

The 2D code light profiles at the end of the crystal, after undergoing a spatial Fourier transform according to the Fraunhofer diffraction equation, determine the far field pattern.[4] Since this calculation is reversible, it is possible to calculate from a given far field pattern the light behavior at the crystal that must have caused that pattern. We used this fact to place a rectangular window function over the central exiting beam of green light to extract its time profile (Figure 3), a process that will hereafter be referred to as *windowing*.

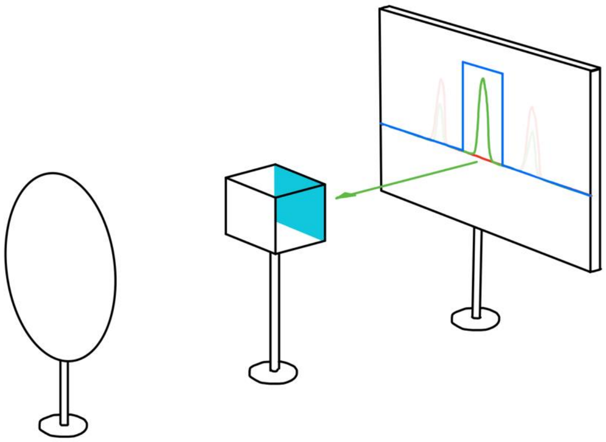

Figure 3. Far field pattern windowed to central peak, pictorial. Windowing the central green beam provides information about the behavior of green light at the crystal's exit surface and enables extraction of the green beam's time profile.

2.2 Test cases

We conducted qualitative comparisons between the 1D and 2D outputs, examining the time profile of the green beam exiting the end of the crystal. For a temporally dispersed pulse, we compared outputs when the 2D code's beams were collinear, non-collinear and non-windowed, and non-collinear and windowed. The following parameters were used for the example test from this research shown in the results section (Table 1 and Table 2).

Table 1. Photoinjector input parameters.

Crystal type	Beta barium borate (BBO)
Crystal angle	23.2999°
Crystal length	1 mm
Pulse duration (FWHM)	330 fs, each pulse
Pulse energy	20 μJ, each pulse
Lens focal length	3 m
Beam offsets, non-collinear	±10 mm
Initial beam $1/e^2$ radius	1 mm, each pulse

Table 2. Beam phase shifts.

	2^{nd} order	3^{rd} order
Beam A	3.27 ps^2	-0.42 ps^3
Beam B	-3.27 ps^2	0.42 ps^3

3. Results and discussion

For the case of dispersion, we first begin with the 1D output. Recall that the 1D code calculates SFG between the two beams but does not account for SHG within the beams. Figure 2 shows result of this calculation; the plot depicts the time intensity profile of green light exiting the crystal and was the basis for comparison with the 2D code outputs.

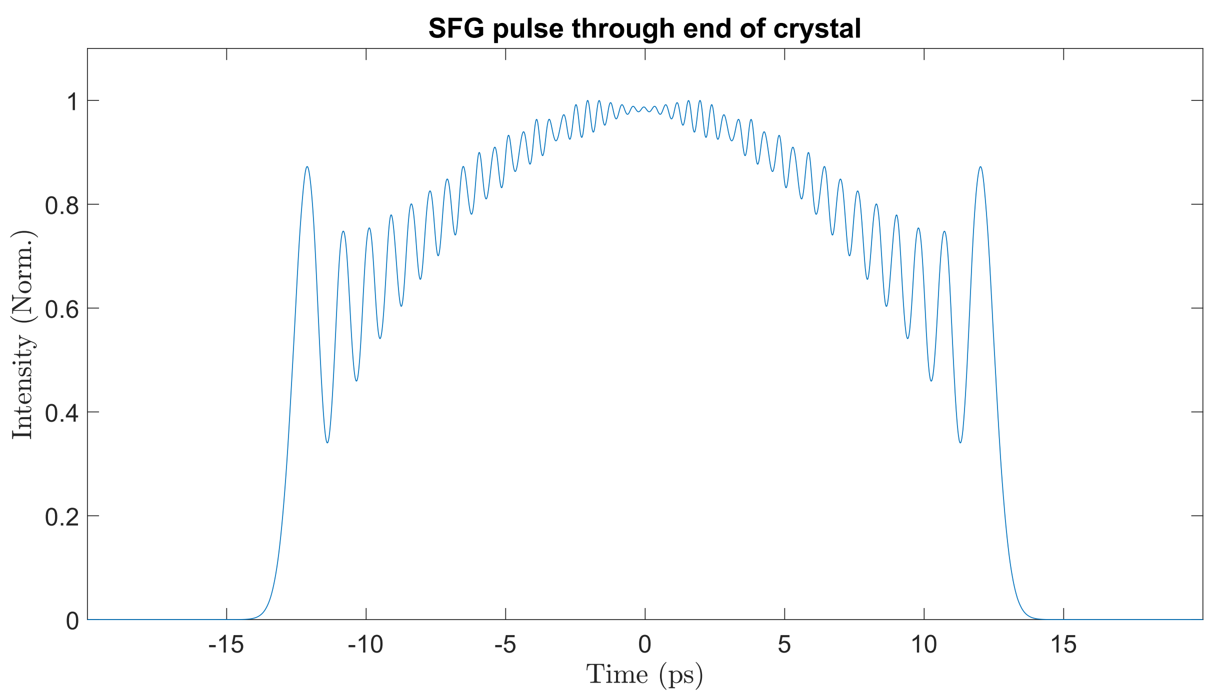

Figure 4. Time profile of green light at exit surface of crystal, 1D code. This corresponds to the central beam that exits the first crystal and enters the spectral filter in Figure 1. This provided a source of comparison for verifying the results of the 2D model.

There were three cases for comparison in the 2D code: collinear input beams, non-collinear non-windowed, and non-collinear windowed.

In Figure 5, the simulation results for these three cases are shown. Row 1 shows the far field pattern, and Row 2 shows the light behavior back calculated from the far field pattern; the plots in Row 2 depict the intensity profile of light with respect to time at each point along the end of the crystal's horizontal plane. Row 3 shows the time profile at the central x-step only, which is the time profile of the central green beam.

It is immediately apparent that the non-collinear windowed case matches the 1D pattern while the collinear and non-collinear non-windowed cases show very strong distortion. Without windowing, we see light from all three green beams overlapping in the crystal, and this interference obscures the central beam's time profile. However, with the central beam windowed, the interference effects are removed, and the time profile matching the 1D is clear, as seen in Row 3 Column 3. Windowing was therefore crucial to visualizing the true time profile of the central beam in the 2D model.

It is important to note that all of these plots have been normalized for intensity. The current models of the code produce outputs with differing intensities, and there is ongoing investigation into the cause of and solution to this discrepancy.

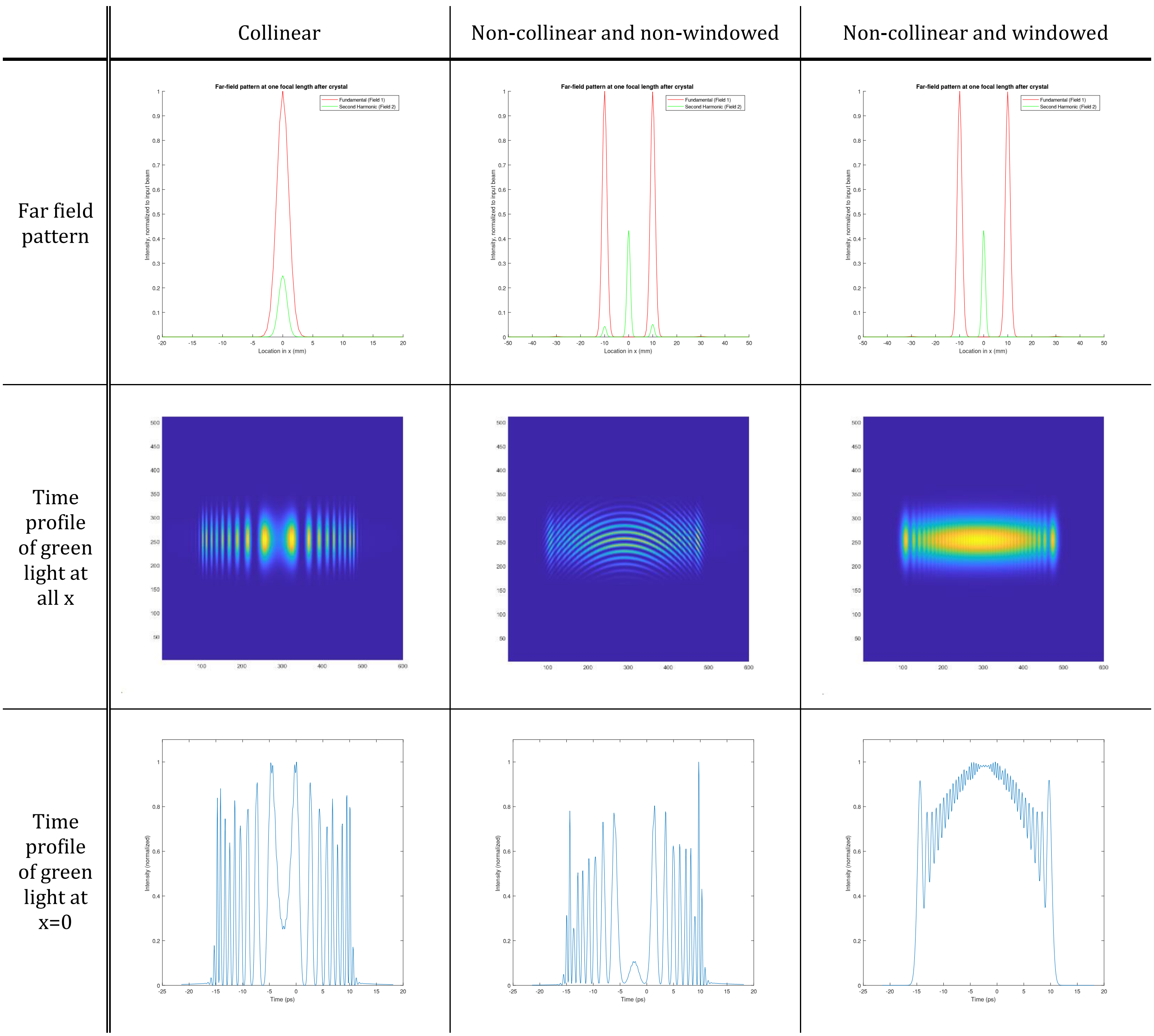

Figure 5. 2D simulation results for the three cases. Columns 1-3 respectively contain outputs for the collinear, non-collinear non-windowed, and non-collinear windowed cases. Rows 1-3 respectively depict the far field pattern, the time intensity profiles of green light exiting the crystal at all transverse locations, and that of the green light at only the central transverse location (the result of slicing the Row 2 plots horizontally at their midpoint). Interference fringes are visible in the plots at Row 2 Column 1 and Row 2 Column 2, which cause the large oscillations seen in the corresponding graphs below. However, that interference is not present in Column 3 due to windowing.

4. Conclusions

4.1 Summary of results

The prior 1D MATLAB simulation of this portion of the photoinjector did not represent many aspects of the true system; namely, it used collinear beams and only calculated for sum frequency generation (SFG). The 2D MATLAB model included a lens to create non-collinear incidence on the crystal and included both second harmonic generation (SHG) and SFG. Only when modeling in 2D were we able to see the interference effects of the two mixing beams. However, the presence of this interference obscured the time profile of the central green beam of interest. Then, only when we segmented the far field pattern to the central beam were we able to see that the 1D and 2D green beam time profiles indeed matched.

4.2 Future work

The shapes arising from the 1D and 2D models are similar, but the intensities do not match. This error is the result of differing normalization methods of the initially generated pulses. We have not yet determined the best way to rectify the issue.

Once that issue is resolved, we hope to make inputs more flexible; at the moment, only two beams are able to enter the lens, and the pulses of the two beams must have the same parameters. We would like to be able to apply separate parameters to each input beam and possibly increase the number of input beams entering the lens.

We also plan to make this model compatible with models of other photoinjector components to create a more comprehensive simulation. With the entire system modeled, machine learning algorithms can be developed to tune the photoinjectors parameters to those that will produce the best X-rays for the LCLS's experiments. This is the overarching objective of this work and its parallel constituents.

Acknowledgements

This work was supported in part by the U.S. Department of Energy (DOE), Office of Science, Office of Workforce Development for Teachers and Scientists (WDTS) under the Science Undergraduate Laboratory Internships (SULI) program. My thanks go to the DOE for providing this research opportunity, and to Dr. Enrique Cuellar and Rebecca Flores for facilitating SLAC's participation in the program.

I extend utmost gratitude to Dr. Sergio Carbajo and Randy Lemons for their mentorship and guidance and to fellow SULI student Melina Endsley for her work in this collaborative effort. Last but not least, this project would not be complete without the adjacent research performed by Jack Hirschman and SULI students Amy McKeown-Green and Rose Knight.

References

[1] "LCLS Overview." SLAC National Accelerator Laboratory, Stanford University.

[2] Lemons, Randy, et al. "Next-generation of photoinjectors for linear accelerators and x-ray free electron lasers." Presented at SPIE Photonics West, 2021.

[3] Paschotta, Rüdiger. "Pulse propagation modeling." RP Photonics Encyclopedia, RP Photonics Consulting GmbH.

[4] Voelz, David G. *Computational Fourier Optics: A MATLAB Tutorial.* SPIE, 2011.